

Flux-creep activation energy for a $\text{BaFe}_{1.9}\text{Ni}_{0.1}\text{As}_2$ single crystal derived from alternating current susceptibility measurements

Jun-Yi Ge,^{1,a)} Lin-Jun Li,^{2,3} Zhu-An Xu,³ and Victor V. Moshchalkov¹

¹INPAC—Institute for Nanoscale Physics and Chemistry, KU Leuven, Celestijnenlaan 200D, B-3001 Leuven, Belgium

²Advanced 2D Materials and Graphene Research Center, National University of Singapore,

2 Science Drive 2, Singapore 117546

³Department of Physics, Zhejiang University, Hangzhou 310027, China

(Received 19 January 2016; accepted 18 April 2016; published online 29 April 2016)

Systematic ac susceptibility measurements have been performed to investigate the vortex dynamics in a $\text{BaFe}_{1.9}\text{Ni}_{0.1}\text{As}_2$ single crystal as a function of temperature, frequency, ac field amplitude, and dc magnetic field. The complex activation energy $U(T, B, j)$ is derived in the framework of thermally activated flux creep theory and can be expressed in one simple formula. A power law dependence of $U \sim B^\alpha$ with $\alpha = -0.46$ is observed. The activation energy reaches 10^4 K at low fields, suggesting strong pinning in the material. The nonlinear function of the activation energy vs. the current density is determined, which has the expression of $U \propto j^{-0.1}$. Published by AIP Publishing.

[<http://dx.doi.org/10.1063/1.4948356>]

INTRODUCTION

In type-II superconductors, magnetic field can penetrate into the material in the form of quantized vortices,¹ which is important for maintaining superconductivity at high magnetic fields. However, in the presence of flowing current density j , perpendicular to the external field B , energy dissipation takes place due to the motion of vortices under the influence of the Lorentz force $\mathbf{F}_L = \mathbf{j} \times \mathbf{B}$. The dissipation directly leads to finite resistance, thus Joule heating is generated and superconductivity is destroyed.² To solve this problem, pinning centers are introduced to the superconductors. By trapping vortices with pinning centers, critical current can be dramatically enhanced. Examples of pinning centers include ion-irradiated point defects,³ grain boundaries,⁴ thickness variations,⁵ atom vacancies,⁶ lithographically introduced antidots,^{7,8} and so on.

The iron-based superconductors (IBSs) discovered in 2008 have attracted intense interest.⁹ On the fundamental side, IBS provides a new platform to study high temperature superconductivity and its mechanism, which has been an intriguing issue for scientific community for nearly three decades. On the other hand, the very high critical fields,¹⁰ high critical current,¹¹ and their metallic parent phases make IBS very promising for technological applications. In our previous study, we have shown that the critical current density reaches 10^7 A/cm² in single crystalline sample of the 122-phase,¹² suggesting strong intrinsic pinning in the material. However, the origin of the strong pinning is not clear so far. An alternate way to investigate the pinning mechanism is by studying the vortex motion activation energy U of the superconductors. The activation energy determines the crossover, above which vortices overcome the attractive force exerted by the pinning centers and dissipation appears. Therefore, it is essential to study the activation energy against vortex motion in order to shed the light on the pinning mechanism.

Among many ways to study the activation energy, the ac susceptibility measurements have the advantage of high sensitivity and acquiring information in a much shorter time window (10^{-5} – 10^{-1} s), which is important when studying the vortex dynamics in superconductors.^{13–20} Also, the applied small ac field will not alter the original vortex lattice, while in the standard transport measurements, the vortex lattice can experience a reorganization due to the Lorentz force of the applied current.²¹

In this paper, by using ac susceptibility measurements, we study in detail the vortex dynamics in an optimally doped high quality $\text{BaFe}_{1.9}\text{Ni}_{0.1}\text{As}_2$ single crystal at different ac fields, frequencies, and dc fields. The complex dependence of activation energy as a function of temperature, magnetic field, and current density is determined, which can be well expressed by one self-consistent formula. Our results shed new light on the understanding of the pinning mechanism in iron-based superconductors.

EXPERIMENTAL

The studied single crystal was prepared using self flux method as reported in Ref. 22. The sample has a mirror-like surface which can be easily cleaved. Room temperature X-ray diffraction (XRD) was measured on a D/Max-rA diffractometer with Cu K_α radiation. Only [001] direction is observed, indicating that c-axis is perpendicular to the cleaved surface. The sample, with a size of $\sim 1.5 \times 2.0 \times 0.3$ mm³, is characterized by $T_c = 20.1$ K, $\Delta T_c = 1.1$ K (10%–90% criterion) as shown in Fig. 1(a) by both dc and ac magnetization measurements. The ac susceptibility measurements were performed using a Quantum-Design physical properties measurement system with the external dc field up to 8 T and an ac field with the amplitude and frequency in the range of $h_{ac} = 0.5$ –12 Oe and 133–9777 Hz, respectively. Both dc and ac fields are perpendicular to the sample surface (ab-plane) in all the measurements.

^{a)}Junyi.Ge@fys.kuleuven.be

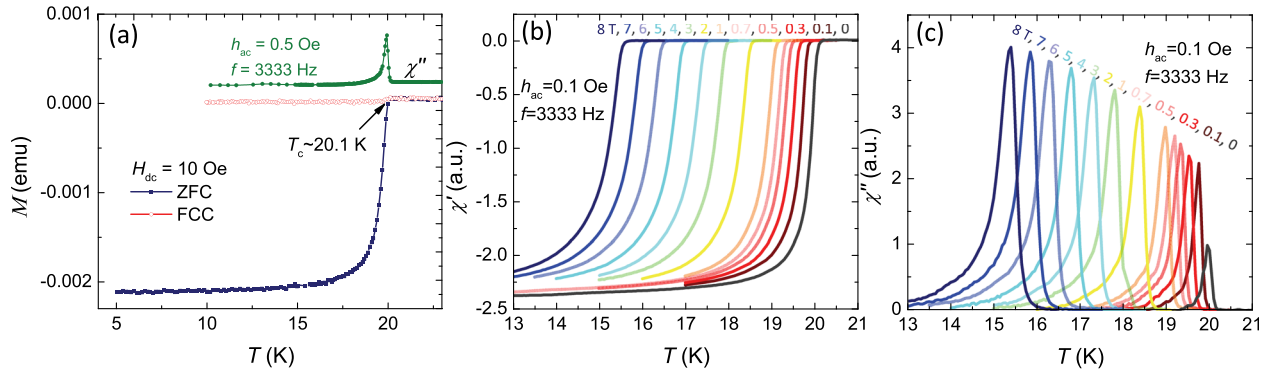


FIG. 1. (a) Temperature dependence of magnetization in field-cooling and zero-field-cooling mode in the external field of $H_{dc} = 10$ Oe, showing a sharp drop at $T_c = 20.1$ K. The out-of-phase ac susceptibility at $h_{ac} = 0.5$ Oe and $f = 3333$ Hz is also shown which exhibits a narrow dissipation peak below T_c . Temperature dependence of in-phase (b) and out-of-phase (c) of ac susceptibility measured under various dc magnetic fields at $h_{ac} = 0.1$ Oe and $f = 3333$ Hz.

RESULTS AND DISCUSSION

The ac susceptibility has been used to study the vortex dynamics in other iron-based superconductors, e.g., 1111-family¹⁷ and 122-family.^{19,23} It is known that the in-phase ac susceptibility exhibits a sharp decrease at T_c , while at lower temperatures the out-of-phase shows a dissipation peak at T_p due to the melting of the vortex lattice.

Figures 1(b) and 1(c) present the temperature dependence of the in-phase and out-of-phase ac susceptibility under various dc fields, respectively. As dc field increases, the transition temperature shifts to lower temperatures, while the transition width (δT_c) remains almost constant. The relatively small δT_c and its almost H -independent behavior suggest the high quality of our sample. To study the complex activation energy U , the thermally activated flux creep model is used,¹⁶ where the activation energy can be expressed as

$$U(T_p, B_{dc}, j) = G(T_p)E(B_{dc})F(j) = T_p \ln \frac{1}{f t_0}, \quad (1)$$

where $G(T_p)$, $E(B)$, and $F(j)$ account for the temperature, magnetic field, and current density dependence of U , respectively. t_0 is the characteristic microscopic time scale.

Numerical simulations have shown that, during the penetration of the ac field into a superconductor, the static critical state model (Bean model) can be used.²⁴ The magnetic field profile inside the sample can be regarded as a straight line. At

the peak temperature T_p , where the flux front reaches the center of the sample, the current density can be estimated using

$$j = h_{ac}/d, \quad (2)$$

where $2d$ is the thickness of the slab sample.

It is clear from Eq. (1) that, at a constant h_{ac} (i.e., constant current density) and B_{dc} , a plot of $\ln f$ versus $G(T_p)/T_p$ should give a straight line with the slope of $U(j, B_{dc}) = E(B_{dc})F(j)$. By varying B_{dc} while keeping h_{ac} constant, one can get the field dependence of the activation energy $E(B)$, and vice versa. In order to rule out the memory effect of flux dynamics,¹⁹ all the measurements were performed by cooling down the sample from above T_c .

Fig. 2(a) presents some typical curves of the temperature dependence of the out-of phase ac susceptibility under various frequencies at $B_{dc} = 5$ T and $h_{ac} = 8$ Oe. As the frequency decreases, the peak position shifts to lower temperatures. This is reasonable considering that the vortices have more time for relaxation at a lower frequency, resulting in full penetration at lower temperatures. Similar behavior has also been observed in other superconducting systems, which is explained in terms of flux creep.^{16,25} The effect of ac amplitude on the flux dynamics at each frequency is also measured at various dc magnetic fields. This allows us to determine the activation energy as a function of current density and external field. In total, up to 252 curves of temperature dependence of ac susceptibility are measured.

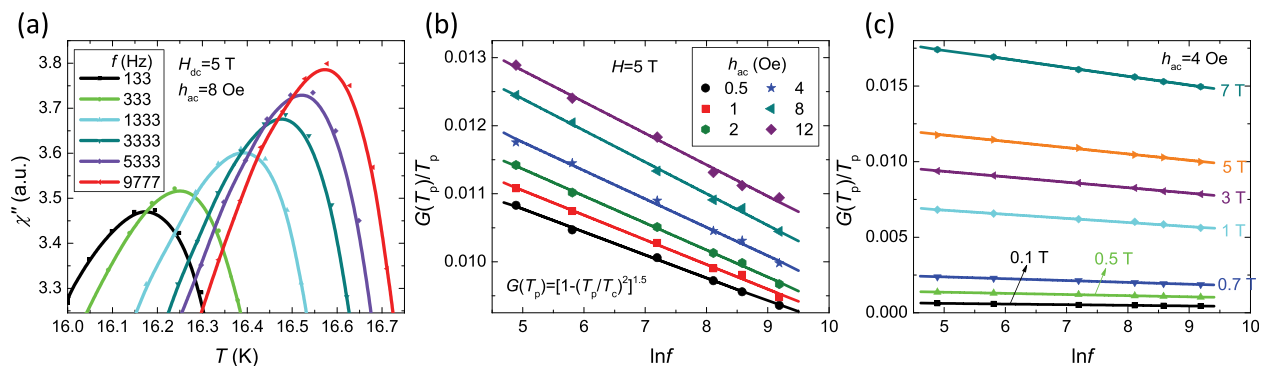


FIG. 2. (a) Temperature dependence of out-of-phase ac susceptibility at $B_{dc} = 5$ T, $h_{ac} = 8$ Oe, and f varying from 133 Hz to 9777 Hz. (b) Frequency dependence of $G(T_p)/T_p$ measured at various ac fields (current densities) under dc magnetic field of 5 T. (c) $G(T_p)/T_p$ vs. $\ln f$ at various dc magnetic fields as indicated in the panel for $h_{ac} = 4$ Oe. In both (b) and (c), the solid lines are linear fits to the data.

Another feature that needs to be determined is the temperature dependence of the activation energy. It has been found that the activation energy cannot be regarded as an isothermal parameter due to the large variation of the T_p as a function of frequency. In our measurements, ΔT_p reaches up to 1 K. Therefore, the explicit temperature dependence of U must be taken into account.^{23,26} According to Ref. 27, $G(T)$ has the following form:

$$G(T) \equiv [1 - (T/T_c)^r]^n, \quad (3)$$

where r and n , determined by the experiments, are fitting parameters to make the $G(T_p)/T_p$ vs. $\ln f$ straight lines at all the fields. Here, by adjusting $r=2$ and $n=1.5$, we have found that the Arrhenius law is valid for our experimental data. Such approach has also been used to account for the $G(T)$ in $\text{HgBa}_2\text{Ca}_2\text{Cu}_3\text{O}_x$ ^{28,29} and $\text{TlSr}_2\text{Ca}_2\text{Cu}_3\text{O}_y$ ¹⁵ materials.

Fig. 2(b) shows the semi-log plot of f vs. $G(T_p)/T_p$ at various ac fields, corresponding to different current densities, for $H=5$ T. The straight lines are linear fitting to the data as discussed above. The activation energy $U(j, B_{dc}=5 \text{ T})$ can be derived from the slopes of the straight lines. In analogy to Fig. 2(b), by repeating the temperature dependence of ac susceptibility measurements at various external fields, the dc field dependence of activation energy at each fixed current density can also be derived from the plot of $\ln f$ vs. $G(T_p)/T_p$, for example, as shown in Fig. 2(c) for $h_{ac}=4$ Oe. The perfect linear fitting of the experimental data at various dc and ac magnetic fields suggests that the chosen temperature dependence of activation energy works well for our sample. From the fitting, it is also possible to get the value of t_0 (e.g., 2.5×10^{-9} s for $H_{dc}=0.1$ T and $h_{ac}=4$ Oe), which is reasonable.

The derived activation energy, representing the effective pinning barrier, as a function of external magnetic field is plotted in Fig. 3. The activation value at low fields reaches 10^4 K, comparable with the value observed in other iron-based superconductors, such as $\text{SmFeAsO}_{0.8}\text{F}_{0.2}$ ($\sim 5 \times 10^4$ K),¹⁷ $\text{Ba}_{0.72}\text{K}_{0.28}\text{Fe}_2\text{As}_2$ ($\sim 10^4$ K),³⁰ $\text{K}_{0.8}\text{Fe}_2\text{Se}_2$ ($\sim 6 \times 10^5$ K),²³ and $\text{FeTe}_{0.5}\text{Se}_{0.5}$ ($\sim 10^3$ – 10^4 K).^{31,32} Such high value suggests strong pinning in the material. By scaling the experimental data by $j^{-0.1}$ to take account for the current density dependence of the activation energy, all the data collapse to one

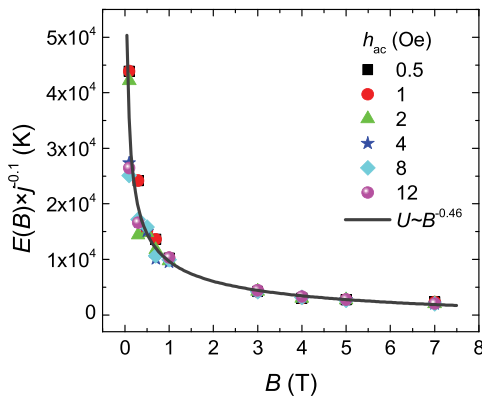


FIG. 3. The activation energy $U \propto E(B_{dc}) \times j^{-0.1}$ as a function of the magnetic field for $\text{BaFe}_{1.9}\text{Ni}_{0.1}\text{As}_2$ at various current densities. The solid line is the fitting curve of $U \propto B^{-0.46}$. Clearly, all the data collapse on the fitting curve very well.

universal curve which can be well fitted by using $U \propto B^{-0.46}$. It has been found that, in both cuprates and 1111-family of iron-based superconductors, a field dependence of $U \sim B^\alpha$ with low α characterizes for the single vortex pinning,^{17,33} i.e., the number of vortices is lower than the number of pinning centers. At relatively high fields, $U \sim B^{-1}$ is often observed due to the collective pinning response of vortices.¹⁸ In the current study, the observed index of $\alpha = -0.46$ in the whole measured field regime (up to 8 T) suggests that neither single vortex pinning nor collective pinning could account for the vortex pinning landscape. The most plausible applicable mechanism here might be a strong plastic pinning which predicts a $\sim B^{-0.5}$ dependence with the magnetic field.³⁴ The relatively weak field dependence of U in $\text{BaFe}_{1.9}\text{Ni}_{0.1}\text{As}_2$ in a broad field range is important for possible applications of this material.

Following from Eqs. (1) and (2), the current density dependence of activation energy is shown in Fig. 4. We have found that, by scaling the data by $B^{-0.46}$, all the data collapse around the curve which has the dependence of $F(j) \propto j^{-\beta}$ with $\beta = 0.1 \pm 0.02$. Here, the relative bigger discrepancy for the index might arise from the complex distribution of current density inside the superconductor, which is rather difficult to clarify explicitly with ac magnetization measurements. The magnetic field dependence is consistent with the one derived in Fig. 3. Also, the observed $F(j)$ is consistent with the one derived from the scaling shown in Fig. 3. The self-consistent scalings of $U(j, B)$ in Figs. 3 and 4 suggest that the complex expression of activation energy in Eq. (1) is quite reasonable. Therefore, the temperature, field, and current density dependent activation energy can be expressed as

$$U(T, B, j) = U_0 \left[1 - \left(\frac{T}{T_c} \right)^2 \right]^{1.5} \left(\frac{B_0}{B} \right)^\alpha \left(\frac{j_0}{j} \right)^\beta, \quad (4)$$

where U_0 , B_0 , and j_0 are scaling parameters and the exponents α and β are determined to be 0.46 and 0.1, respectively.

The observed power law dependence of $U \sim j^\beta$ has been predicted from the collective pinning theory with the exponent β depending on the dimensionality of the problem and

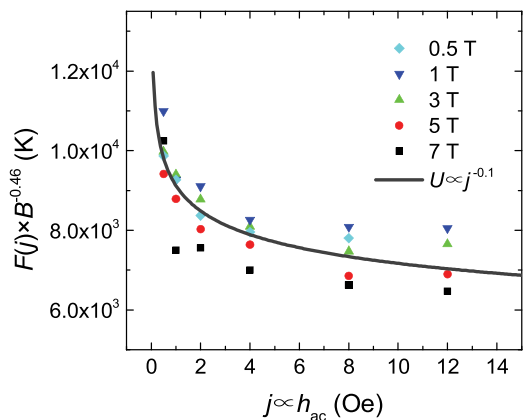


FIG. 4. The activation energy $U \propto F(j) \times B^{-0.46}$ as a function of the magnetic field for $\text{BaFe}_{1.9}\text{Ni}_{0.1}\text{As}_2$ at various external fields. The solid line is the fitting curve of $U \propto j^{-0.1}$.

on the particular regime of the flux creep.³⁵ Similar index values ($\beta = -0.11$) have also been reported in organic superconductors.³⁶

CONCLUSION

In summary, detailed ac susceptibility measurements have been performed to study the flux dynamics in an optimally doped $\text{BaFe}_{1.9}\text{Ni}_{0.1}\text{As}_2$ single crystal. The complex activation energy has been determined by using one universal expression which provides deep insight in understanding the pinning mechanism in iron-based superconductors. The activation energy reaches 10^4 K at low fields and follows the trend $\sim B^{-0.46}$ in a large field region, indicating very strong pinning. The current density dependence of activation energy is determined to be $\sim j^{-0.1}$.

ACKNOWLEDGMENTS

The work at KU Leuven was supported by the FWO, the Methusalem Funding by the Flemish Government, and the MP1201 COST Action.

- ¹J.-Y. Ge, J. Gutierrez, V. N. Gladilin, and V. V. Moshchalkov, *Nat. Commun.* **6**, 6573 (2015).
- ²Y. B. Kim, C. F. Hempstead, and A. R. Strnad, *Phys. Rev.* **139**, A1163 (1965).
- ³N. Haberkorn, B. Maiorov, I. O. Usov, M. Weigand, W. Hirata, S. Miyasaka, S. Tajima, N. Chikumoto, K. Tanabe, and L. Civale, *Phys. Rev. B* **85**, 014522 (2012).
- ⁴C.-L. Song, Y.-L. Wang, Y.-P. Jiang, L. Wang, K. He, X. Chen, J. E. Hokman, X.-C. Ma, and Q.-K. Xue, *Phys. Rev. Lett.* **109**, 137004 (2012).
- ⁵A. Bezryadin, Y. N. Ovchinnikov, and B. Pannetier, *Phys. Rev. B* **53**, 8553 (1996).
- ⁶J. C. Phillips, *Phys. Rev. Lett.* **72**, 3863 (1994).
- ⁷M. Baert, V. V. Metlushko, R. Jonckheere, V. V. Moshchalkov, and Y. Bruynseraede, *Phys. Rev. Lett.* **74**, 3269 (1995).
- ⁸V. V. Moshchalkov, M. Baert, V. V. Metlushko, E. Rosseel, M. J. Van Bael, K. Temst, Y. Bruynseraede, and R. Jonckheere, *Phys. Rev. B* **57**, 3615 (1998).
- ⁹Y. Kamihara, T. Watanabe, M. Hirano, and H. Hosono, *J. Am. Chem. Soc.* **130**, 3296 (2008).
- ¹⁰E. Mun, N. Ni, J. M. Allred, R. J. Cava, O. Ayala, R. D. McDonald, N. Harrison, and V. S. Zapf, *Phys. Rev. B* **85**, 100502 (2012).
- ¹¹Q. P. Ding, Y. Tsuchiya, S. Mohan, T. Taen, Y. Nakajima, and T. Tamegai, *Phys. Rev. B* **85**, 104512 (2012).
- ¹²J. Li, J. Yuan, Y. H. Yuan, J. Ge, M. Y. Li, H. L. Feng, P. J. Pereira, A. Ishii, T. Hatano, A. V. Silhanek *et al.*, *Appl. Phys. Lett.* **103**, 062603 (2013).
- ¹³L. Fabrega, J. Fontcuberta, S. Pinol, C. J. van der Beek, and P. H. Kes, *Phys. Rev. B* **47**, 15250 (1993).
- ¹⁴C. J. van der Beek, V. B. Geshkenbein, and V. M. Vinokur, *Phys. Rev. B* **48**, 3393 (1993).
- ¹⁵S. Y. Ding, G. Q. Wang, X. X. Yao, H. T. Peng, Q. Y. Peng, and S. H. Zhou, *Phys. Rev. B* **51**, 9107 (1995).
- ¹⁶G. Blatter, M. N. Feigelman, V. B. Geshkenbein, A. I. Larkin, and V. M. Vinokur, *Rev. Mod. Phys.* **66**, 1125 (1994).
- ¹⁷G. Prando, P. Carretta, R. De Renzi, S. Sanna, A. Palenzona, M. Putti, and M. Tropeano, *Phys. Rev. B* **83**, 174514 (2011).
- ¹⁸G. Prando, P. Carretta, R. De Renzi, S. Sanna, H. J. Grafe, S. Wurmehl, and B. Buchner, *Phys. Rev. B* **85**, 144522 (2012).
- ¹⁹J. Ge, J. Gutierrez, J. Li, J. Yuan, H.-B. Wang, K. Yamaura, E. Takayama-Muromachi, and V. V. Moshchalkov, *Phys. Rev. B* **88**, 144505 (2013).
- ²⁰J. Ge, J. Gutierrez, J. Li, J. Yuan, H.-B. Wang, K. Yamaura, E. Takayama-Muromachi, and V. V. Moshchalkov, *Appl. Phys. Lett.* **104**, 112603 (2014).
- ²¹A. V. Silhanek, M. V. Milosevic, R. B. G. Kramer, G. R. Berdiyrov, J. Van de Vondel, R. F. Luccas, T. Puig, F. M. Peeters, and V. V. Moshchalkov, *Phys. Rev. Lett.* **104**, 017001 (2010).
- ²²L. J. Li, Y. K. Luo, Q. B. Wang, H. Chen, Z. Ren, Q. Tao, Y. K. Li, X. Lin, M. He, Z. W. Zhu, G. H. Cao, and Z. A. Xu, *New J. Phys.* **11**, 025008 (2009).
- ²³J. Ge, J. Gutierrez, M. Li, J. Zhang, and V. V. Moshchalkov, *Appl. Phys. Lett.* **103**, 052602 (2013).
- ²⁴C. P. Bean, *Phys. Rev. Lett.* **8**, 250 (1962).
- ²⁵J. J. Qin and X. X. Yao, *Phys. Rev. B* **54**, 7536 (1996).
- ²⁶S. Sengupta, D. Shi, Z. Wang, M. E. Smith, and P. J. McGinn, *Phys. Rev. B* **47**, 5165 (1993).
- ²⁷M. E. McHenry, S. Simizu, H. Lessure, M. P. Maley, J. Y. Coulter, I. Tanaka, and H. Kojima, *Phys. Rev. B* **44**, 7614 (1991).
- ²⁸S. Y. Ding, J. Li, H. M. Shao, J. W. Lin, C. Ren, and X. X. Yao, *Phys. Rev. B* **53**, 900 (1996).
- ²⁹M. J. Qin, X. L. Wang, S. Soltanian, A. H. Li, H. K. Liu, and S. X. Dou, *Phys. Rev. B* **64**, 060505(R) (2001).
- ³⁰X.-L. Wang, S. R. Ghorbani, S.-I. Lee, S. X. Dou, C. T. Lin, T. H. Johansen, K.-H. Muller, Z. X. Cheng, G. Pelecekis, M. Shabazi, A. J. Qviller, V. V. Yurchenko, G. L. Sun, and D. L. Sun, *Phys. Rev. B* **82**, 024525 (2010).
- ³¹E. Bellingeri, S. Kawale, I. Pallecchi, A. Gerbi, R. Buzio, V. Braccini, A. Palenzona, M. Putti, M. Adamo, E. Samelli, and C. Ferdeghini, *Appl. Phys. Lett.* **100**, 082601 (2012).
- ³²J. Ge, S. Cao, S. Shen, S. Yuan, B. Kang, and J. Zhang, *Solid State Commun.* **150**, 1641 (2010).
- ³³E. Bartolome, A. Palau, A. Llordes, T. Puig, and X. Obradors, *Phys. Rev. B* **81**, 184530 (2010).
- ³⁴V. M. Vinokur, M. V. Feigelman, V. B. Geshkenbein, and A. I. Larkin, *Phys. Rev. Lett.* **65**, 259 (1990).
- ³⁵M. V. Feigelman, V. B. Geshkenbein, A. I. Larkin, and V. M. Vinokur, *Phys. Rev. Lett.* **63**, 2303 (1989).
- ³⁶A. E. Primenko, V. D. Kuznetsov, V. V. Metlushko, N. D. Kushch, and E. B. Yagubskii, *Zh. Eksp. Teor. Fiz.* **107**, 649 (1995).